

Volume Title
*ASP Conference Series, Vol. **Volume Number***
Author
 © ***Copyright Year*** *Astronomical Society of the Pacific*

Magnetic braking in convective stars

Gaitee A.J. Hussain

*ESO, Karl-Schwarzschild-Str. 2, Garching bei München, 85748
 Germany*

Abstract.

Magnetic braking causes the spin-down of single stars as they evolve on the main sequence. Models of magnetic braking can also explain the evolution of close binary systems, including cataclysmic variables. The well-known period gap in the orbital period distribution of cataclysmic variable systems indicates that magnetic braking must be significantly disrupted in secondaries that are fully convective. However, activity studies show that fully convective stars are some of the most active stars observed in young open clusters. There is therefore conflicting evidence about what happens to magnetic activity in fully convective stars.

Results from spectro-polarimetric studies of cool stars have found that the field morphologies and field strengths are dependent on spectral type and rotation rate. While rapidly rotating stars with radiative cores show strong, complex magnetic fields, they have relatively weak dipole components. Fully convective stars that are rapidly rotating also possess strong magnetic fields, but their configurations are much simpler; often close to dipole fields.

How this change in field geometry affects the stellar wind is the focus of several ongoing modelling efforts. Initial results suggest that rapidly rotating active dwarfs drive much stronger winds, about two orders of magnitude larger than those on the Sun.

1. Introduction

The idea of stellar magnetic fields driving angular momentum loss can be dated back to the 1962 paper by Evry Schatzman. This paper brought together the ideas of the day to describe how the Hertzsprung-Russell diagram can be split into distinct sections. Stars with slow rotation rates are in the lower right part of the diagram – they are predominantly stars with outer convective envelopes. As convective stars host solar-type dynamo activity, stellar magnetic fields keep material in the extended magnetosphere in corotation, thus exerting a braking torque and driving the spin-down of a single star on the zero age main sequence.

Magnetic braking should therefore operate in all systems with low mass stars ($0.4 < M_* < 1.5 M_{\odot}$); i.e., stars with outer convective envelopes. Magnetic braking in the low mass secondary star of close binary systems is also responsible for determining binary separations. The secondary loses angular momentum and angular momentum is then removed from binary systems through tidal locking, causing the binary separation to decrease and evolve further (Mestel 1968).

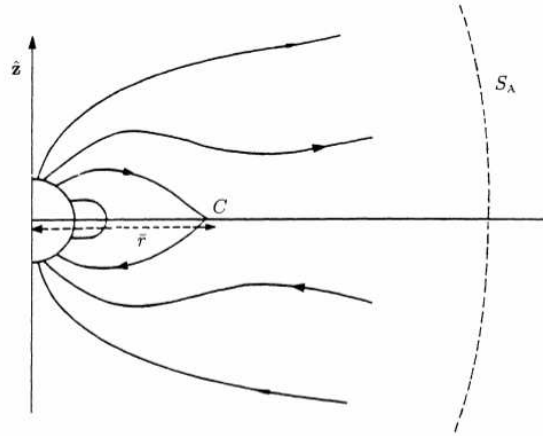


Figure 1. A schematic diagram of the wind model of Mestel and Spruit (1987). Here C marks a position inside the “dead zone” while the Alfvén surface, S_A , denotes the start of the “wind zone” where the field is radial. This figure has been reproduced from Campbell (1997) with permission.

The first observational evidence for magnetic braking was gathered from a rotation study of G-dwarfs in open clusters of different ages (e.g., Pleiades, Hyades) and in the field. The seminal paper by Skumanich (1972) found that these stars spin down following the inverse square root of their age, $v \sim t^{1/2}$. This braking law was adopted to derive magnetic braking laws for close binary stars with cool secondaries, assuming that secondary stars have a comparable mass loss rate to that of single G stars (Verbunt & Zwaan 1981). However, it is worth noting that the Skumanich results are based only on G stars with $v_e \sin i$ values up to 30 km/s. Close binary stars can far exceed these velocities.

This early work led to the development of a variety of angular momentum loss formulations. Initially braking laws were developed assuming symmetric winds flowing along purely radial field lines (Weber & Davis 1967, Mestel 1968). Later formulations of braking laws allow for a more complex two-component coronal structure with an inner closed region and an outer region in which field lines are open (Figure 1; Mestel 1984, Kawaler 1988, Mestel and Spruit 1987, Tout and Pringle 1992, Ivanova and Taam 2003). Solar eclipse images provide support for this large-scale coronal model as a first approximation.

In these later models, the star has a large-scale dipole field that causes a “dead zone” near the equator in which field lines are closed. As matter is trapped in this zone, it cannot escape or contribute to the angular momentum loss and reduces the efficiency of the magnetic braking. The hot expanding corona is driven by thermal pressure gradients and centrifugal acceleration and causes the formation of an outer zone (the “wind zone”) where the field is open.

The field of the star gets distorted where the kinetic energy density of the outflowing material matches the poloidal magnetic field density. Field lines are blown open into the flow where the poloidal velocity matches the Alfvén speed; where the kinetic energy density matches the poloidal magnetic energy density.

This can be calculated using the poloidal magnetic field, B_{pol} and the mass density, ρ :

$$v_A = \frac{B_{pol}}{\sqrt{(\mu_o \rho)}}. \quad (1)$$

Other variations are possible: Tout and Pringle (1992) propose a stellar field that declines more strongly with distance due to more complex stellar fields; they also assume that not all open field lines connect with the whole stellar surface. Ivanova and Taam (2003) assume that the X-ray luminosity of the secondary star is generated in the dead zone and therefore use X-ray observations of stars to model the volume of the dead zone. Just by this modification they find that their magnetic braking prescription can reproduce the observed rotation rates at a range of masses. It is clear that the field configuration is important in determining basic properties of the dead zone and where the wind zone starts. X-ray measurements alone cannot reveal the distribution of the underlying field geometry.

There are numerous published angular momentum braking laws; these all rely on a series of assumptions that have been treated differently. Knigge et al. (2011, *this volume*) demonstrate most effectively how these laws differ, and in fact can predict opposite trends with orbital period and stellar mass. We clearly need to understand more about the nature of stellar magnetic braking from observations of convective stars.

2. Rotational evolution of stars: observations

Stellar winds (or outflows) are very difficult to detect directly in main sequence cool stars. On the Sun the wind causes a mass-loss rate of $\dot{M} = 2 \times 10^{-14} M_{\odot} \text{ yr}^{-1}$ (e.g., Feldman et al. 1977). However, its low density and high temperature make it difficult to detect. Direct measurements of outflows on other main sequence stars are even more challenging.

Indirect measurements can be made through observations of the interaction between the stellar wind and the local interstellar medium. This is detected as extra Ly α absorption in UV spectra from the *Hubble Space Telescope*, HST (Wood et al. 2002, 2005). HST studies of a handful of systems reveal that mass loss rates should scale with magnetic activity. However, the scaling relation depends on very few systems, some of which are binaries and therefore not well understood.

Studies of close binary systems and cool stars have been conducted to characterise mass loss and angular momentum loss rates further. These are described below. While the techniques differ a coherent picture is starting to emerge.

2.1. Magnetic braking in cataclysmic variable systems (CVs)

Magnetic braking has been shown to explain the evolution of close binary systems. All close binary systems lose angular momentum through gravitational radiation. The angular momentum loss rate due to gravitational radiation should depend on the mass of the component stars, M_1 and M_2 and the orbital sepa-

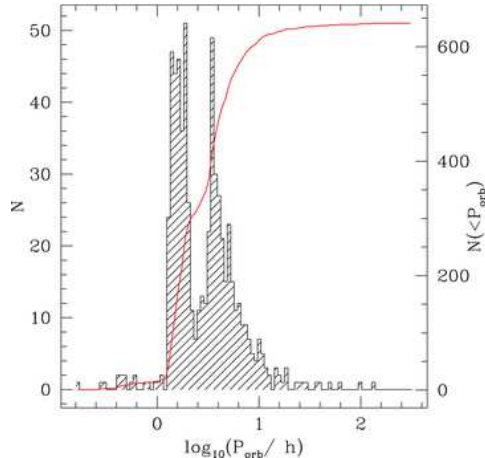


Figure 2. Orbital period distribution of cataclysmic variable binary systems. There are few systems with periods between 2-3 hours. This is attributed to a disruption in magnetic braking as stars become fully convective. Reproduced from Davis et al. (2008) with permission.

ration a , as follows (Paczynski 1967, Knigge et al. 2011):

$$dJ_{GR}/dt \sim \frac{M_1^2 M_2^2 M^{1/2}}{a^{7/2}}. \quad (2)$$

Gravitational radiation clearly weakens in systems with large orbital separations. The observed mass transfer rates in long period cataclysmic variable binary and low mass X-ray binary systems can only be explained by another angular momentum loss mechanism (Verbunt & Zwaan 1981). This is attributed to magnetic braking, with the assumption that convective stars in close binary systems will show the same magnetic braking levels as those seen in single convective stars. Their magnetic braking law prescription depends on the secondary mass, M_2 , radius, R_2 and rotation, Ω as shown below:

$$dJ_{MB}/dt \sim M_2 R_2^4 \omega^3. \quad (3)$$

The orbital period distribution of CVs is shown in Figure 2 (Davis et al. 2008). This has a largely bimodal distribution, with very few systems in the so-called “gap” between orbital periods of 2-3 hours. In order to explain the accretion rates and sizes of the donor stars observed above the period gap, it is necessary to invoke magnetic braking. At orbital periods of 3 hours secondary stars become fully convective and presumably this causes its magnetic activity to be disrupted and essentially switches off the magnetically driven wind (outflow). As magnetic braking switches off, the donor shrinks within its Roche lobe, mass transfer is shut off and the secondary re-attains thermal equilibrium. The system is then no longer observed as a cataclysmic variable and subsequent orbital evolution of the CV is driven by gravitational radiation only. Mass transfer resumes again when the secondary star makes contact with its Roche lobe once more at $P_{orb} \sim 2h$.

An important proof of this scenario is provided in Patterson et al (2005). They find that the masses of the donor stars above and below the period gap are very similar, which is expected if mass transfer is reduced so the masses remain largely unchanged. In line with the magnetic braking scenario, donor stars above the period gap are more inflated than those below the period gap. New work measuring the sizes of the donor stars further supports these findings: Knigge et al. (2011) fit the sizes of the secondaries using a parametrised version of the Verbunt & Zwaan braking law (Rappaport et al. 1983). They find that gravitational radiation losses alone are also not sufficient to account for the star sizes below the period gap, with twice the level of gravitational radiation-driven braking required to explain the evolution below the period gap.

2.2. Magnetic braking in post common envelope binary systems (PCEBs)

Studies of PCEBs can shed light on the nature of magnetic braking. If magnetic braking changes with secondary mass, the timescales for the onset of accretion in close binaries should be affected. Politano & Weiler (2006) use a Monte Carlo population synthesis code to investigate the relative distribution of PCEBs with low mass and high mass secondaries assuming different magnetic braking formulations.

They find the most noticeable effect when magnetic braking is completely disrupted in fully convective stars; this causes a significant decline in PCEB secondaries with radiative cores. The relative number of PCEBs declines by 38% in the mass bin at which magnetic braking is switched on ($M_2 > 0.37 M_\odot$). Intermediate braking prescriptions are also investigated, in which the magnetic braking is reduced in rapidly rotating systems or the most X-ray active stars. However, for both of the intermediate braking cases they find that the numbers of low mass and high mass secondaries remains similar. The fourth case investigated assumes no magnetic braking, this finds a relative increase in the number of PCEBs with increasing secondary mass.

A large survey of white dwarf-main sequence (WDMS) binaries using the SDSS finds a decline of about 80% in the *relative fraction* of PCEBs at masses greater than $M_2 > 0.37 M_\odot$ (Schreiber et al. 2010). However, the simulation above predicts the *relative number* of PCEBs not the fraction of PCEB/WDMS systems: the number of WDMS binary systems should increase with secondary mass. Taking this into account, Politano & Weiler’s predictions translate to a decrease of between 38–73% in the fraction of PCEB/WDMS systems at higher masses. Schreiber et al. (2010) caution that, while the decrease they observe with increasing secondary star mass is in general agreement with the predictions from the disrupted magnetic braking model, the observed distribution is broader than that predicted. A contributing factor may be the uncertainty in the spectral type determination of these systems, which would effectively broaden an initially steep function. Alternatively, the onset of the disruption of magnetic braking may occur more gradually rather than at one mass.

3. Magnetic activity and braking in single stars

Since Skumanich’s 1972 study of G main sequence stars, we now have a wealth of information tracking the angular momentum properties of convective stars

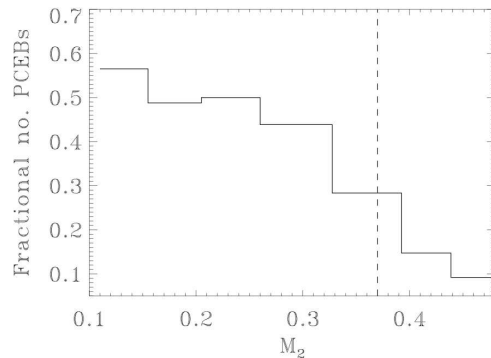


Figure 3. The fractional number of PCEB systems ($n_{\text{PCEB}}/n_{\text{WDMS}}$) relative to the total number of white dwarf main sequence star systems as a function of secondary mass, M_2 (adapted from Schreiber et al. 2010). The dashed line denotes the fully convective boundary.

over a range of spectral types (i.e. masses) and ages. Barnes (2003) collate rotation periods from open cluster studies and find that the braking timescales depend strongly on a star’s spectral type, age, and crucially, the type of magnetic activity behaviour displayed in that star.

He finds that stars ostensibly fall into two activity tracks: the more slowly rotating stars lie on the interface track, I : so-called as they show signs of classic interface (solar-type) dynamo activity. They spin-down with age efficiently following a modified version of the Skumanich law. The other track is called the convective track, C : this tends to contain the more magnetically active, rapidly rotating stars and shows a reduced braking efficiency. Expressions governing the spin-down rates of single stars on these two tracks are shown below (Barnes & Kim 2010), where k_C and k_I are constants and τ_c is the convective turnover timescale:

$$\frac{dJ}{dt} = -\Omega I_c k_C / \tau_c ; \text{ for the convective stars,} \quad (4)$$

$$\frac{dJ}{dt} = -\Omega^3 I_* 2\tau_c / k_I ; \text{ for the interface stars.} \quad (5)$$

Stars move from the C track to the I track as they age, with lower mass stars taking longer to make this transition. Almost all G stars will have made this transition by the first 200 Myr on the main sequence, while M stars can take over 500 Myr.

4. Key questions

Our current understanding of angular momentum evolution comes predominantly from statistical studies of cool star systems. The root cause of the magnetic braking mechanism is of course the stellar magnetic field. We can learn about the properties of stellar magnetic fields in more detail by studying

proxies of magnetic activity such as X-ray emission. More recently, tomographic techniques have revealed even more detailed information about the distribution and characteristics of magnetic fields at the surfaces of stars where they first emerge. In the rest of this paper we address the following questions. These have been posed by earlier studies and serve to place our understanding of the root causes of magnetic braking and stellar winds on a solid footing.

1. What is the dependence of stellar magnetic fields on spectral type, age, rotation and binarity?
2. What happens to magnetic fields in fully convective stars?
3. Do magnetic fields look similar in single stars and in their binary star counterparts?
4. How does the stellar wind depend on the stellar magnetic field?

5. Magnetic fields in cool stars

Magnetic braking laws that have been developed for convective stars rely on simple prescriptions for the stellar magnetic field, which has been variously modelled as a dipole or even as a monopole in some early cases.

The magnetic activity state of a star is often characterised using a magnetic activity proxy, e.g., X-ray and Ca II H&K emission. These are measures of the magnetic heating in the outer atmospheres of cool stars and, therefore, indirect measures of the magnetic flux threading through the stellar atmosphere. Numerous X-ray studies of open clusters have revealed that X-ray luminosity and therefore magnetic activity levels are strongly dependent on rotation rate, with X-ray emission generally increasing with increasing rotation. A tighter correlation is found with the Rossby number, $R_o = P_{\text{rot}}/\tau_c$; where P_{rot} = stellar rotation period and τ_c = convective turnover time-scale. τ_c is a theoretical quantity that increases with increasing convection zone depth.

X-ray and Ca II activity studies have found that the dynamo does *not* in fact switch off at full convection, as predicted by studies of the evolution of close binary systems. Indeed, fully convective stars have similar fractional X-ray luminosities (L_X/L_{bol}) to active G and K stars (Figure 4; Pizzolato et al. 2003, James et al. 2000, Jeffries et al. 2011). Furthermore, there is still considerable uncertainty regarding exactly how these measures of magnetic heating relate to the underlying magnetic field. While these diagnostics may be sensitive to the magnetic energy levels in stars, they cannot reveal the underlying magnetic geometry and therefore the conditions that drive stellar winds. How magnetic flux is distributed in these stars is central to understanding the conditions driving stellar winds.

5.1. Spot maps

The technique of Doppler imaging has been used to image the surfaces of over 80 convective stars since it was first introduced in 1987 by Vogt, Penrod & Hatzes (see review by Strassmeier 2009). It can only be applied to rapidly rotating stars with $v_e \sin i > 15\text{km/s}$; these stars are some of the most magnetically active,

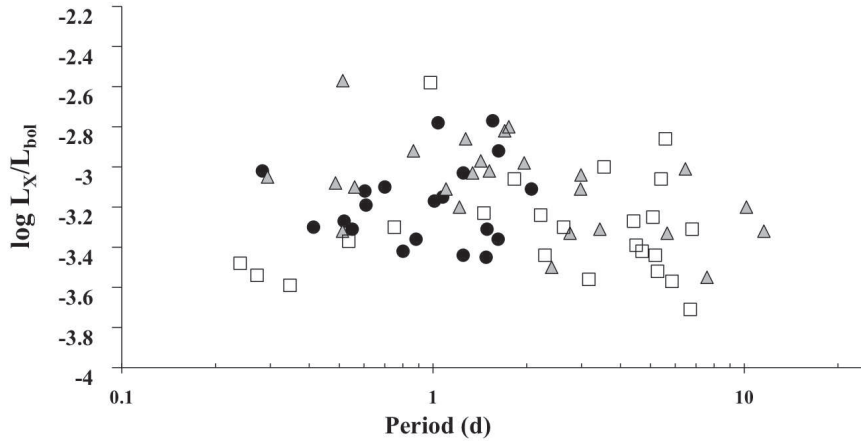


Figure 4. Fractional X-ray luminosity as a function of rotation period for stars with different masses ($M_* < 0.37 M_\odot$: circles; $0.38 < M_* < 0.55$: grey triangles; $0.55 < M_* < 1.0 M_\odot$: open squares). The filled circles are fully convective systems and show no clear drop in X-ray luminosity (i.e. no drop in magnetic activity) Adapted from Jeffries et al. (2011).

displaying X-ray luminosities up to two orders of magnitude greater than that on the Sun. The dark starspots that are reconstructed are analogous to sunspots, which mark the largest concentrations of magnetic flux at the solar surface.

Surface spot maps show that stars with similar spectral types and rotation rates have similar spot patterns, suggesting that they not only have similar levels of activity but also similar magnetic flux emergence patterns. Figure 5 shows Doppler maps from four K1-2 main sequence stars with similar activity levels – all of these maps show polar/high latitude spots co-existing with low latitude spots. Most G and K dwarfs tend to possess high latitude spots, with many showing large spots that cover their poles – also known as polar caps (e.g., Donati & Collier Cameron 1997, Barnes et al. 2005, Jeffers et al. 2011). G and K stars often have a mixture of both high latitude/polar spots and low latitude spots. In early M dwarfs, that are not fully convective the starspot patterns change, with little evidence for polar spots (Barnes et al. 2004).

The K2 secondary in the post common envelope binary, V471 Tau, is of particular interest. It is instructive to compare this map with those of single stars with similar masses and rotation rates, such as AB Dor in Figure 5. As V471 Tau has an inclination angle of nearly 90° the low latitude spots cannot be reconstructed accurately and are smeared out due to a mirroring effect between the northern and southern hemispheres of the star. Despite this V471 Tau’s spot maps suggest that there are shorter lived low latitude spots co-existing with the polar cap. This spot pattern is typical of other active K dwarfs and suggests that binarity and tidal locking do not fundamentally change the magnetic field generation mechanism in stars (Hussain et al. 2006). Our study of the tidally locked binary system, HD 155555 (G5 + K0), found spot and magnetic field patterns in the binary component stars that are indistinguishable from those of single stars with similar spectral types (Dunstone et al. 2008).

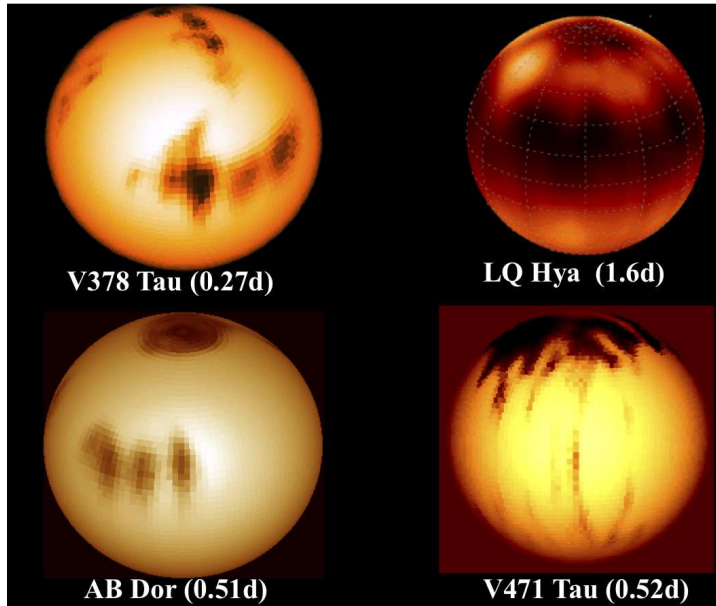


Figure 5. Surface spots on four rapidly rotating K stars with similar magnetic activity levels (Hussain et al., 2000, 2006, Rice & Strassmeier 1998). The rotation periods and names of all four stars are shown as captions. These images are snapshots of the stellar surface at a selected phase.

It is possible to map the surfaces of the secondaries in CV systems using the technique of Roche tomography (Watson & Dhillon (2001), which uses similar principles to those in Doppler imaging techniques. Maps of AE Aqr, BV Cen and over eight other systems have now been published; they show a mixture of high and low latitude spots though it is not clear if these stars host polar spots due to the often low contrast reconstructions. This is a particularly challenging technique as strong irradiation patterns across CV secondary surfaces can dilute the effects of starspots (e.g., QQ Vul; Watson et al. 2003). Furthermore, as CVs have short orbital periods and the secondaries are faint, getting high S/N spectra in short exposure times (to limit phase smearing) limits the numbers of systems that can be studied in this way with current facilities.

5.2. Magnetic field maps

With the advent of high resolution, high throughput spectro-polarimeters (e.g., CFHT-ESPADONS, ESO 3.6m-HARPSpol) we can now detect stellar magnetic fields directly using circular spectro-polarimetry. Time-series of high resolution circularly polarised spectra are inverted to produce surface magnetic field distributions using Zeeman Doppler imaging (Semel 1989, Donati & Brown 1997). This technique applies Doppler imaging principles to high resolution circularly polarised profiles. As circularly polarised spectra are sensitive to the line-of-sight component of the stellar magnetic field, the technique enables us to measure the size of the magnetic field as well as reconstructing its geometry and distribution across the stellar surface.

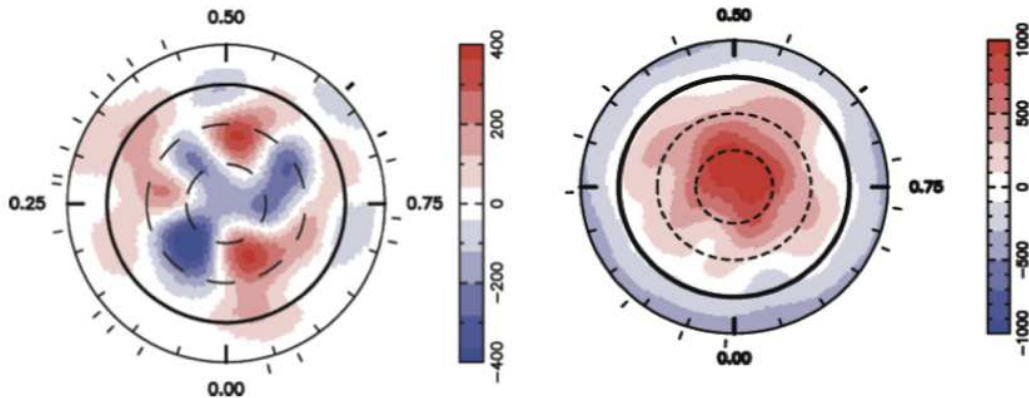


Figure 6. Across the fully convective boundary: radial field maps of the surfaces of two M stars (Donati et al. 2008, Morin et al. 2008). The colour scale represents magnetic flux in G. Left: DT Vir ($M_{0.5}$, $P_{\text{rot}} = 2.9$ d) Right: EQ Peg B ($M_{4.5}$, $P_{\text{rot}} = 0.4$ d)

Over 30 convective stars have been imaged using Zeeman Doppler imaging, covering a range of spectral types, rotation rates and evolutionary states. A summary of recent results was presented in the review by Donati & Landstreet (2009; see their Figure 3). Studies show two clear transitions in magnetic activity characteristics. The first happens with rotation rate: slowly rotating G and K-type stars possess simple, mainly axisymmetric poloidal fields. In more rapidly rotating stars, the field strengths increase and surface azimuthal fields – horizontal, East-West oriented fields – strengthen. The second transition in magnetic activity occurs in fully convective stars as described below.

5.2.1. The transition to full convection

Magnetic field maps of M dwarfs show a marked change with mass. While high mass M stars look similar to G and K-type stars, fully convective M stars ($M_* \leq 0.4 M_{\odot}$) have predominantly poloidal field topologies that are more axisymmetric; they also have stronger fluxes than their higher mass counterparts (Figure 6; Donati et al. 2008, Morin et al. 2008). This ties in with X-ray studies, which find no significant drop in X-ray luminosity of fully convective stars (Figure 4).

A more complete picture of magnetic field properties of convective stars is obtained by combining the field topologies from magnetic maps with measurements of mean magnetic fluxes measured from intensity spectra. Because circularly polarised spectra are only sensitive to the line-of-sight component of the magnetic field, multiple switches in polarity across the surface cause the circularly polarised signature to be diluted due to flux cancellation. Measurements of Zeeman broadening in intensity profiles of magnetically sensitive lines make it possible to measure the mean magnetic flux at the surface of a star (e.g., Johns-Krull & Valenti 2000, Reiners & Basri 2009).

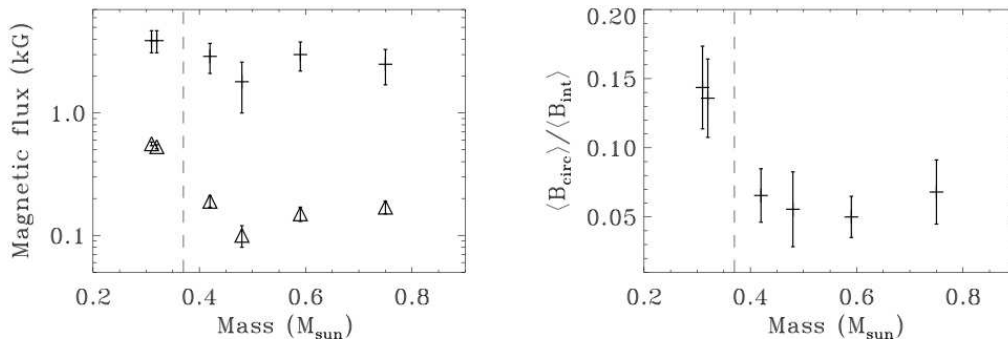


Figure 7. Magnetic fields in M stars with different masses (Reiners & Basri 2009, adapted with permission here). *Left:* Mean magnetic fluxes recovered from intensity diagnostics (crosses) and circularly polarised profiles (triangles). Circular polarisation recovers less flux overall than intensity; as circular polarisation is sensitive to the line-of-sight component of the stellar magnetic field, complex topologies will lead to flux cancellation. The mean magnetic fluxes from intensity, $\langle B_{\text{int}} \rangle$ (crosses), do not change significantly with stellar mass. The dashed line denotes the fully convective boundary. *Right:* The fractional flux from circularly polarised profiles increases in fully convective stars, as their simpler magnetic field topologies result in reduced flux cancellation.

Reiners & Basri (2009) compare their measurements of mean magnetic flux for stars covering a range of masses, $0.31 \leq M_* \leq 0.75$. Their results are summarised in Figure 7. They find that the mean magnetic flux $\langle B_{\text{int}} \rangle$ is unaffected by the transition to full convection. However, the size of the magnetic flux recovered from circularly polarised spectra ($\langle B_{\text{circ}} \rangle$ in Figure 7) rises. This suggests that the field polarities must be simpler and less prone to flux cancellation at lower masses, thus supporting the results from Zeeman Doppler imaging studies.

6. Wind models for cool stars

Surface magnetic field maps can be extrapolated to produce detailed models of a star’s magnetosphere. The surface field maps are used to define the locations of footpoints of fields that extend in to the star’s corona and beyond (Hussain et al. 2002). A co-ordinated X-ray and Zeeman Doppler imaging study of the K star, AB Dor, showed that the coronal model created by extrapolating the surface magnetic field map could reproduce the level of rotational modulation observed in the contemporaneous X-ray lightcurves and spectra (Hussain et al. 2007).

Recent studies have shown how similar maps can be used to model stellar winds in detail using magnetohydrodynamic codes that were originally developed for the Sun (Cohen et al. 2010, Vidotto et al. 2011). These studies use the BATS-R-US code, and require the surface magnetic fluxes as an input, assuming

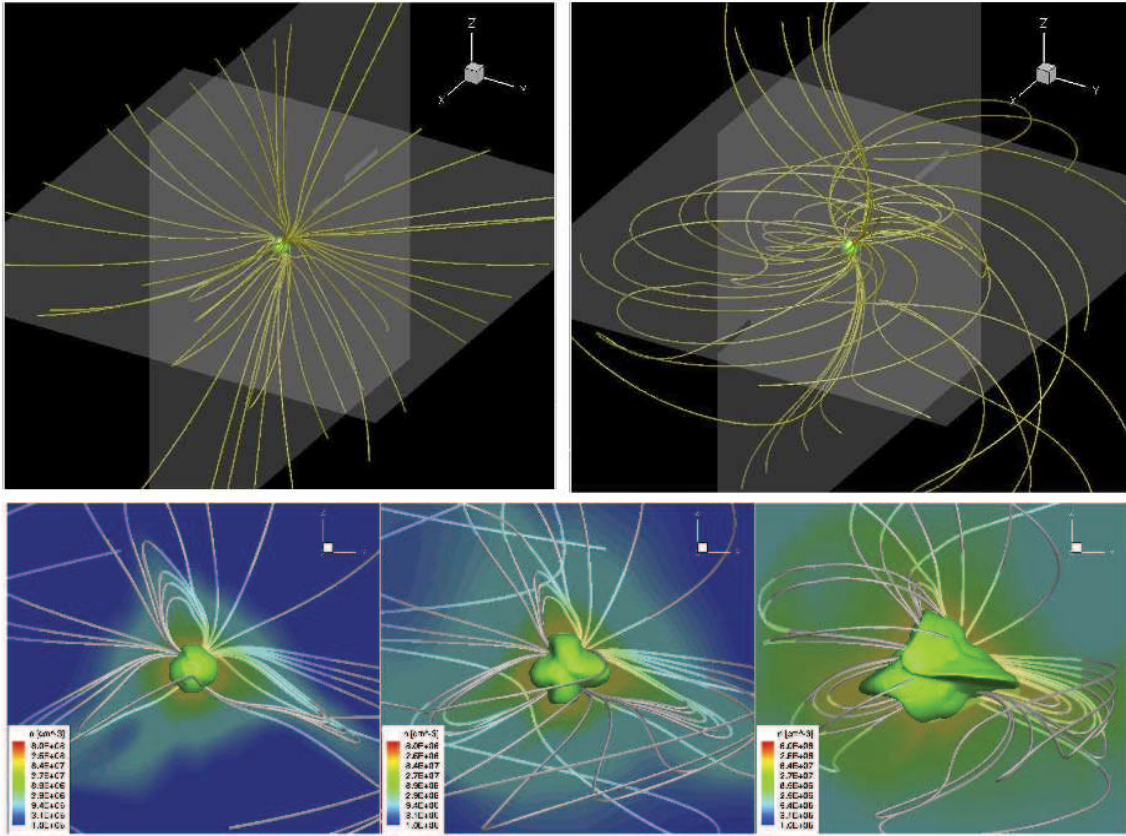


Figure 8. *Top:* The effect of increasing P_{rot} on the stellar magnetosphere. Spinning up AB Dor from $P_{\text{rot}} = 25$ d (top left) to the actual $P_{\text{rot}} = 0.5$ d results in greater field tangling. *Bottom:* The effect of increased base coronal density from left to right, $n_o = 2 \times 10^8$, 10^9 and 10^{10}cm^{-3} . The iso-surface of $n = 10^8 \text{cm}^{-3}$ is shown in green and the colour scale represents the density ($1E6$ to $8E8 \text{cm}^{-3}$) (Cohen et al. 2010, with permission).

a potential field initially. Further inputs are the star’s parameters and values for the base coronal density, ρ_o and temperature, T_o . The code assumes a thermal wind and allows the wind to evolve and interact with the magnetic field in a self-consistent way until a steady-state wind solution is reached. The interaction between the coronal density structure and the speed of the wind determines the angular momentum loss rate (\dot{J}) and the mass loss rate (\dot{M}) for the star.

We find that wind models of the rapidly rotating K0 star, AB Dor ($P_{\text{rot}} = 0.5$ d, $T_{\text{eff}} = 5000\text{K}$), indicate significantly higher mass loss rates than those seen on the present-day Sun (Cohen et al. 2010). AB Dor’s surface maps show a complex field distribution, with field strengths of over 700 G, much of which is concentrated at higher latitudes than on the Sun. These models require the base coronal density as an input. This is inherently uncertain even though it can be estimated from X-ray coronal diagnostics, which are likely somewhat higher than the density at the base of the wind. We use values ranging between

$n_o = 2 \times 10^8$ and 10^{10}cm^{-3} to investigate the dependence of the star on this parameter.

Our simulations show that two factors affect the loss rates of the stars (Figure 8):

a) Rotation rate – increasing AB Dor’s rotation period by a factor of 50 (from $P_{\text{rot}}=0.5$ d to 25 d) reduces the loss rate by up to $\dot{J}_{0.5}/\dot{J}_{25} \sim 70$ and $\dot{M}_{0.5}/\dot{M}_{25} \sim 10$. AB Dor’s maps show strong high latitude flux near the pole of the star. This combined with rapid rotation results in the tangling of field lines and thus more of the corona is closed, leading to larger loss rates than in slower rotators with similar magnetic field distributions. If the star is spun down more of the field becomes open and the loss rates are reduced considerably.

b) Coronal base density – an increase of a factor of 50 ($n_0 = 2 \cdot 10^8$ to 10^{10}cm^{-3}) increases the loss rates by over an order of magnitude ($\dot{J}_{10^{10}}/\dot{J}_{10^8} \sim 10$ and $\dot{M}_{10^{10}}/\dot{M}_{10^8} \sim 20$). This is because greater mass at the base increases the mass flux through the closed “dead zone”; this decreases the density gradient with height, which effectively leads to a greater torque on the rotating star.

An analogous study of the mid-M star, V374 Peg (M4, $P_{\text{rot}}=0.44$ d), finds similarly large loss rates (Vidotto et al. 2011). V374 Peg’s surface field is quite similar to that of EQ Peg A (Figure 6): it has a simple, largely dipolar field, with a strength of 1660 G (compared to only 1-2 G on the Sun). While the mass and angular momentum loss rates are similar to those predicted for AB Dor, the reasons are different. The models for V374 Peg show much faster winds than on AB Dor, with relatively little field tangling despite the rapid rotation and presumably due to the simple dipolar field in V374 Peg. As with the AB Dor study, Vidotto et al. also find that the braking rate strongly depends on the coronal base density, which is not well-defined.

These first detailed wind modelling studies pose some interesting questions as they find that braking is more efficient in rapidly rotating stars, including the simpler M dwarf fields. So how do we explain the observations, which suggest that, in fully convective M stars, the braking must become less efficient? Future studies will reveal much more about how mass loss and angular momentum loss rates change with magnetic topology. The wind modelling techniques should first be fine-tuned against the few observable quantities such as the mass loss measurements made by Wood et al. (2005) in a handful of systems.

7. Summary

This review provides an overview of angular momentum evolution in both binary and single star systems. A wealth of observations suggest that magnetic braking is likely to operate at all spectral types. However the form of the magnetic braking changes with spectral type, rotation rate and activity state. The fundamental processes controlling the magnetic braking efficiency have, as yet, to be firmly established. Surface imaging studies of activity in cool stars have revealed a promising avenue and go some way towards answering the key questions we pose in this paper.

1. What is the dependence of stellar magnetic fields on spectral type, age, and rotation?

Clear changes are seen with spectral type and rotation rate. Magnetic field maps of G-M-type stars confirm that the magnetic field topology in active rapidly rotating G and K-type stars differs compared to less active slowly rotating counterparts. Rapidly rotating stars show stronger, more complex, fields; with strong flux typically at high latitudes. Slowly rotating stars have more axisymmetric, simpler dipolar fields with much weaker field strengths.

2. What happens to magnetic fields in fully convective stars?

Magnetic field studies find a transition in M stars near the fully convective boundary ($M_* \leq 0.4 M_\odot$): they possess simpler more axisymmetric dipolar fields of the type seen in slowly rotating stars, but with field strengths up to three orders of magnitude larger. This transition agrees well with where the radiative core becomes negligibly small and convective turnover timescales are expected to increase (Donati et al. 2008). These results are consistent with X-ray and Ca II studies, which cannot detect changes in magnetic topology and find that the magnetic heating in the upper atmospheres of these stars does not switch off or decrease at full convection.

How the change in field topology affects the properties of the stellar wind has yet to be established and is the focus of intensive modelling efforts. Early results from spectro-polarimetric studies of very low mass stars suggest that the field topologies change again below masses of $0.15 M_\odot$: the magnetic field becomes weaker and complex (Morin et al. 2008). However, this requires further investigation as it is based on a small sample and one exception, WX UMa, has been found.

3. Do magnetic fields look similar in single stars and in their binary star counterparts?

Spot and magnetic field maps of the tidally locked main sequence secondaries in binary systems, V471 Tau and HD 155555, look similar to those of single G and K-type stars, with strong flux at both high and low latitudes. Images of secondaries in CVs also suggest a mix of high and low latitude spots. However, the tomography of CV secondaries is very challenging as the spot signatures are difficult to resolve in contrast to irradiation patterns. The direct comparison with main sequence stars of similar masses has yet to be done systematically.

4. How does the stellar wind depend on the stellar magnetic field?

Initial results suggest that rapidly rotating active dwarfs drive stronger winds than those in more slowly rotating systems. This ties in well with observed mass loss rates. However, further work is needed to establish how changes in coronal topology directly affect the angular momentum and mass loss rates in stars. Inputs that are used in these models also should be refined: for example magnetic field maps can be enhanced to account for missing flux from dark polar spots; the base coronal densities also need to be constrained.

Binary evolution studies have established that there is a significant disruption to magnetic braking when stars become fully convective. Ostensibly this transition is congruent with the point at which magnetic field maps show a switch from complex multipolar fields to simple dipolar fields. How strongly this transition should affect magnetic braking has yet to be understood. Rotation studies of single stars indicate that active stars spin down on slower timescales than their inactive counterparts regardless of mass (Barnes 2003, Barnes & Kim 2010); furthermore the braking observed in single stars is weaker than that needed to explain the properties of CV secondaries above and below the period gap (Knigge et al. 2011).

Future avenues of investigation need to address the following points: a) modelling braking in moderately active stars by extrapolating surface magnetic field maps as inputs and refining these models through comparison with the few measurements of loss rates in cool stars; b) once outflows/winds are better understood in single stars models of these winds can be used to investigate the evolution of close binary systems in more detail; c) establishing whether the spot patterns found in CV secondaries are analogous with their counterparts in PCEBs and single stars. Further spot and magnetic field maps from Roche tomography and Doppler imaging studies of close binary systems will prove invaluable to establish this latter point.

Acknowledgments. Linda and the OC's are warmly thanked for the seamless organisation and putting together this enjoyable and stimulating meeting.

8. References

- Barnes, J. R., Collier Cameron, A., Lister, T. A., Pointer, G. R., Still, M. D., 2005, *MNRAS*, 356, 1501
 Barnes, J. R., James, D. J., Collier Cameron, A., 2004, *MNRAS*, 352, 589
 Barnes, S.A., 2003, *ApJ*, 586, 464
 Barnes, S.A., Kim, Y.-C., 2010, *ApJ*, 721, 675
 Campbell, C.G., 1997, *MNRAS*, 291, 250
 Cohen, O., Drake, J. J., Kashyap, V. L., Hussain, G. A. J., Gombosi, T. I., 2010, *ApJ*, 721, 80
 Davis, P. J., Kolb, U., Willems, B., Gänsicke, B. T., 2008, *MNRAS*, 389, 1563
 Donati, J.-F., Collier Cameron, A., 1997, *MNRAS*, 291, 1
 Donati, J.-F., Brown, S.F., 1997, *A&A*, 326, 1135
 Donati, J.-F., Landstreet, J.D., 2009, *ARA&A*, 47, 333
 Donati, J.-F., Morin, J., Petit, P., Delfosse, X., Forveille, T., Aurière, M., Cabanac, R., Dintrans, B., Fares, R., Gastine, T., et al. 2008, *MNRAS*, 390, 545
 Dunstone, N. J., Hussain, G. A. J., Collier Cameron, A., Marsden, S. C., Jardine, M., Stempels, H. C., Ramirez Velez, J. C., Donati, J.-F., 2008, *MNRAS*, 387, 481
 Feldman, W. C., Asbridge, J. R., Bame, S. J., & Gosling, J. T. 1977, in *The Solar Output and its Variation*, ed. O. R. White (Boulder: Colorado Associated Univ. Press), 351
 Hussain, G. A. J., Donati, J.-F., Collier Cameron, A., Barnes, J. R., 2000, *MNRAS*, 318, 961
 Hussain, G. A. J., van Ballegooijen, A. A., Jardine, M., Collier Cameron, A., 2002, *ApJ*, 575, 1078

- Hussain, G. A. J., Allende Prieto, C., Saar, S. H., Still, M., 2006, MNRAS, 367, 1699
- Hussain, G. A. J., Jardine, M., Donati, J.-F., Brickhouse, N. S., Dunstone, N. J., Wood, K., Dupree, A. K., Collier Cameron, A., Favata, F. et al. 2007, MNRAS, 377, 1488
- Ivanova, N., Taam, Ronald E., 2003, ApJ, 599, 516
- James, D.J., Jardine, M.M., Jeffries, R.D., Randich, S., Collier Cameron, A., Ferreira, M., 2000, MNRAS, 318, 1217
- Jeffers, S. V., Donati, J.-F., Alecian, E., Marsden, S. C., 2011, MNRAS, 411, 1301
- Jeffries, R. D., Jackson, R. J., Briggs, K. R., Evans, P. A., Pye, J. P., 2011, MNRAS, 411, 2099
- Johns-Krull, C. M.; Valenti, J. A., 2000, *Stellar Clusters and Associations*, ASP Conf. Proc., Vol. 198. Eds., R. Pallavicini, G. Micela, and S. Sciortino, p.371
- Kawaler, S.D., 1988, ApJ, 333, 236
- Knigge, C., Baraffe, I., Patterson, J., 2011, ApJS, 194, 28
- Mestel, L., 1968, MNRAS, 138, 359
- Mestel, L., 1984, LNP, 193, 49
- Mestel, L., Spruit, H.C., 1987, MNRAS, 226, 57
- Morin, J., Donati, J.-F., Petit, P., Delfosse, X., Forveille, T., Albert, L., Aurière, M., Cabanac, R., Dintrans, B., Fares, R., et al. 2008, MNRAS, 390, 567
- Paczyński, B., 1967, AcA, 17, 287
- Patterson, J., Kemp, J., Harvey, D. A., Fried, R.E., Rea, R., Monard, B., Cook, L. M., Skillman, D.R., Vanmunster, T., Bolt, G., et al., 2005, PASP, 117, 1204
- Pizzolato, N., Maggio, A., Micela, G., Sciortino, S., Ventura, P., 2003, A&A, 397, 147
- Politano, M., Weiler, K.P., 2006, ApJ, 641, 137
- Rappaport, S., Verbunt, F., Joss, P.C., 1983, ApJ, 275, 713
- Reiners, A., Basri, G., 2009, A&A, 496, 787
- Rice, J.B., Strassmeier, K.G., 1998, A&A, 336, 972
- Schatzman. E., 1962, AnAp, 25, 18
- Schreiber, M.R., Gänsicke, B.T., Rebassa-Mansergas, A., et al., 2010, A&A, 513, 7
- Skumanich, A., 1972, ApJ, 171, 565
- Semel, M., 1989, A&A, 225, 456
- Strassmeier, K.G., 2009, A&ARv, 17, 251
- Tout, C.A., Pringle, J.E., 1992, MNRAS, 256, 269
- Verbunt, F., Zwaan, C., 1981, A&A, 100, 7
- Vidotto, A., Jardine, M., Opher, M., Donati, J.F., Gombosi, T.I., 2011, MNRAS, 412, 351
- Vogt, S.S., Penrod, G. D., Hatzes, A. P., 1987, ApJ, 321, 496
- Watson, C. A., Dhillon, V. S., 2001, MNRAS, 326, 67
- Watson, C.A., Dhillon, V. S., Rutten, R., Schwope, A.D., 2003, MNRAS, 341, 129
- Weber, E.J., Davis, L. Jr, 1967, ApJ, 148, 217
- Wood, Brian E., Müller, Hans-Reinhard, Zank, Gary P., Linsky, Jeffrey L., 2002, ApJ, 574, 412
- Wood, B. E., Müller, H.-R., Zank, G. P., Linsky, J. L., Redfield, S., 2005, ApJ, 628, L143